

Rob Horsefield,^{a†} Victoria Yankovskaya,^{b†} Susanna Törnroth,^{c‡} César Luna-Chavez,^{b§} Elizabeth Stambouli,^a James Barber,^a Bernadette Byrne,^a Gary Cecchini,^{b,d,*} and So Iwata^{c,e*}

^aDepartment of Biological Sciences, Imperial College, London SW7 2AZ, England,

^bMolecular Biology Division, Department of Veterans' Affairs Medical Center, San Francisco, CA 94121, USA, ^cDepartment of Biochemistry, BMC, Uppsala University, Box 576, S-751 23 Uppsala, Sweden, ^dDepartment of Biochemistry and Biophysics, University of California, San Francisco, CA 94143, USA, and ^eDepartment of Biological Sciences and Division of Biomedical Sciences, Imperial College, London SW7 2AZ, England

† These authors contributed equally to this work.
‡ Present address: Chalmers University of Technology, Department of Molecular Biotechnology, Lundberg Laboratory, PO Box 462, SE-405 30 Göteborg, Sweden.
§ Present address: Center for Biophysics and Computational Biology, University of Illinois, Urbana-Champaign, IL 61801, USA.

Correspondence e-mail: s.iwata@ic.ac.uk, ceccini@itsa.ucsf.edu

Correspondence e-mail: s.iwata@ic.ac.uk, ceccini@itsa.ucsf.edu

Using rational screening and electron microscopy to optimize the crystallization of succinate:ubiquinone oxidoreductase from *Escherichia coli*

The membrane-bound respiratory complex II, succinate:ubiquinone oxidoreductase (SQR) from *Escherichia coli*, has been anaerobically expressed, then purified and crystallized. The initial crystals obtained were small and diffracted poorly. In order to facilitate structure determination, rational screening and sample-quality analysis using electron microscopy was implemented. The crystals of SQR from *E. coli* belong to the trigonal space group *R*32, with unit-cell parameters $a = b = 138.7$, $c = 521.9$ Å, and diffract to 2.6 Å resolution. The optimization strategy used for obtaining well diffracting SQR crystals is applicable to a wide range of membrane proteins.

Received 8 January 2003
Accepted 22 January 2003

1. Introduction

Succinate:ubiquinone oxidoreductase (SQR; complex II; succinate dehydrogenase), a functional member of both the Krebs cycle and the oxygen respiratory chain, uses electrons derived from the oxidation of succinate for the reduction of ubiquinone. The reduced ubiquinone is utilized by the cytochrome *bc*₁ complex in mitochondria or by ubiquinol oxidase in *Escherichia coli* for the generation of proton motive force across the membrane. SQR is made up of a soluble domain and an integral membrane-anchor domain. The soluble domain comprises two subunits: a flavoprotein (Fp, SdhA), which contains a covalently bound flavin adenine dinucleotide (FAD) cofactor, and an iron-sulfur protein (Ip, SdhB), which contains three distinct iron-sulfur clusters (for a review, see Cecchini *et al.*, 2002). Many SQRs, including the human and *E. coli* enzymes, have membrane-anchor domains composed of two membrane subunits (SdhC and SdhD) which contain one *b*-type haem.

Mutations in human SQR genes can manifest themselves with a wide variety of clinical phenotypes, including optic atrophy, tumour formation, myopathy and encephalopathy (Baysal *et al.*, 2001). In *Caenorhabditis elegans*, the *mev-1* mutant, which has a point mutation in the SdhC subunit, is reported to be hypersensitive to oxygen and to develop a premature ageing phenotype (Ishii *et al.*, 1998).

SQR from *E. coli* can be used as a model to understand the molecular mechanism of these disorders. We have previously reported a hexagonal crystal form diffracting X-rays to 3.5 Å resolution (Törnroth *et al.*, 2002). Owing to the limited resolution and strong anisotropy of the data, we have not been able to obtain a reliable structure using this crystal form. Here,

we present a trigonal crystal form of *E. coli* SQR which diffracts X-rays to 2.6 Å resolution. This paper also addresses how the crystallization conditions were optimized using additives and ultracentrifugation combined with electron-microscopic observation.

2. Materials and methods

2.1. Expression

SQR expression was achieved using *E. coli* strain DW35 transformed with the plasmid pFAS (Maklashina *et al.*, 1998). Endogenous SQR is not expressed in this strain owing to an insertion mutation. The pFAS plasmid (P_{FRD}*sdhCDAB*) encodes the complete SQR coding sequence under the control of the fumarate reductase promoter, which is activated under anaerobic conditions.

DW35 cells transformed with pFAS, grown in LB medium overnight with ampicillin (100 µg ml⁻¹) were used to inoculate 20 l of anaerobic growth media (1:500 dilution). The glycerol-fumarate anaerobic media (Spencer & Guest, 1973) was supplemented with 0.05% (w/v) casamino acids, 0.2% (w/v) tryptone, 0.1% (w/v) yeast extract and 100 µg ml⁻¹ ampicillin. The culture was incubated at 310 K for 18 h with slow stirring. Cells were harvested using continuous-flow centrifugation at 277 K and used immediately for membrane preparation as described previously (Luna-Chavez *et al.*, 2000).

2.2. Purification

Membranes containing 400 mg total protein were resuspended in buffer A (20 mM potassium phosphate, 0.2 mM EDTA pH 7.4) plus Complete protease-inhibitor tablets (Roche,

Indianapolis, USA). A 20% stock solution of the detergent THESIT ($C_{12}E_9$; nona-ethyleneglycol mono-*n*-dodecyl ether; Anatrace, Maumee, OH, USA) was added to give a final detergent concentration of 2% (*w/v*). The suspension was stirred briefly (5 min) at 277 K and then sedimented by centrifugation (100 000*g* for 30 min). The reddish-brown supernatant was filtered through a 0.2 μm nylon filter before chromatographic purification.

The supernatant was applied to a Q-Sepharose Fast Flow 26/10 column (Amersham Biosciences) equilibrated with buffer *B* (20 mM potassium phosphate, 0.2 mM EDTA, 0.05% THESIT pH 7.4). After washing with two bed volumes of buffer *B* and one to two bed volumes of buffer *B* with 100 mM NaCl, the protein was eluted using a gradient of 0.1–0.35 *M* NaCl at a flow rate of 2.5 ml min⁻¹. Fractions containing SQR were concentrated with a Centriprep-30 concentrator (Amicon Inc., Beverly, MA, USA), filtered and diluted with buffer *A* before application to a POROS 50HQ 10/100 column (Perseptive Biosystems, Framingham, MA, USA) equilibrated with buffer *B*. The loading and elution of SQR from the POROS column was identical to that described for the Q-Sepharose column. The fractions containing SQR were concentrated and filtered as above before application to a third column, a Sephacryl S-300 26/60 (Amersham Pharmacia) equilibrated with buffer *C* (20 mM Tris-HCl, 0.05% THESIT pH 7.6). A flow rate of 0.2 ml min⁻¹ was used for separation and the peak fractions containing SQR were collected and concentrated with a Centriprep-30 filter concentrator to a final concentration of ~60 mg ml⁻¹. The sample was filtered through a 0.2 μm filter and used for crystallization trials.

2.3. Initial crystallization

Crystals were grown by the hanging-drop vapour-diffusion method. Protein sample consisting of purified SQR in buffer *C* was mixed in a 1:1 ratio with the reservoir solution and left to equilibrate at 293 K (4 μl total drop volume). Initial crystals were obtained using Hampton Research sparse-matrix crystal screen condition No. 14 with a reservoir solution containing 0.1 *M* Na HEPES pH 7.5, 0.2 *M* CaCl₂ dihydrate and 28% (*v/v*) polyethylene glycol 400. Crystals appeared after 24 h and reached maximum dimensions of 0.05 mm within 72 h.

2.4. Electron microscopy and ultracentrifugation

Protein-sample homogeneity was analyzed using negative-stain electron microscopy. Protein sample was diluted to ~50 $\mu\text{g ml}^{-1}$ with buffer *C* and 5 μl was applied to a carbon-coated Formvar grid (AGAR Scientific), previously glow-discharged for 10 s, and incubated at room temperature for 1 min. Excess sample was blotted away using filter paper and washed twice with water. 2% uranyl acetate was applied to the grid in excess and incubated for 1 min. Excess uranyl acetate was blotted away and the grid was allowed to dry at room temperature. The grid was analyzed using a Philips-CM100 transmission electron microscope (Philips Electron Optics, Eindhoven, The Netherlands) at 80 kV. Following analysis, the preparation process was optimized by a centrifugation step (175 000*g* for

Table 1

Data statistics.

Statistics for the last shell are given in parentheses.	
Data-collection statistics	
Wavelength (\AA)	1.0081
Beam size (μm)	20 × 80
Oscillation range ($^\circ$)	0.5
Exposure time (s frame ⁻¹)	10
Crystal-to-film distance (cm)	197
Data processing and scaling statistics	
Resolution (\AA)	40–2.6 (2.69–2.6)
Unit-cell parameters (\AA)	$a = b = 138.8,$ $c = 521.9$
Total observations	152468
Independent observations	53727
Completeness (%)	89.9 (90.0)
R_{sym} (%)	7.6 (40.8)
$I/\sigma(I)$ †	11.8 (1.58)
V_M ‡§ ($\text{\AA}^3 \text{Da}^{-1}$)	4.08
Solvent content§ (%)	65.9

† $I/\sigma(I)$ is low because of the anisotropy of the diffraction.

‡ Assuming one SQR monomer in the asymmetric unit (Matthews, 1968). § High V_M and solvent content values are common for membrane-protein complexes owing to the detergent micelle surrounding the proteins (Iwata *et al.*, 1998; Ostermeier *et al.*, 1995).

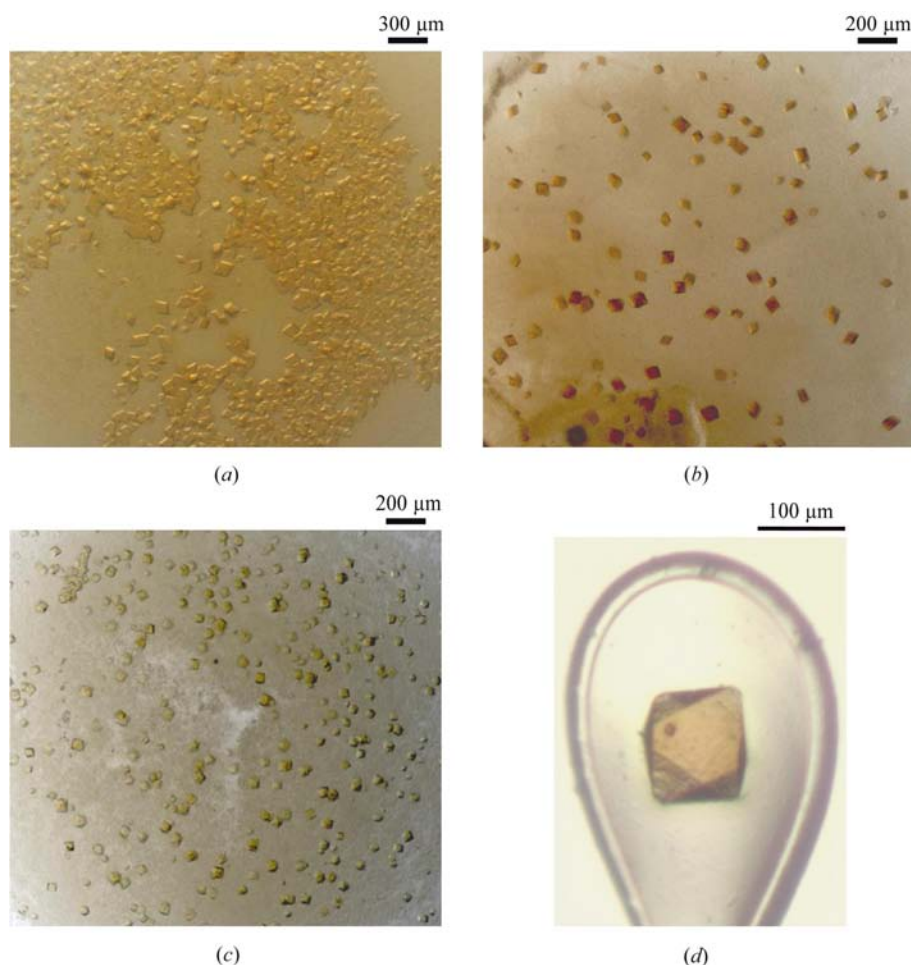


Figure 1

Comparison of crystals obtained from uncentrifuged (*a*) and centrifuged (*b*) protein sample. Far fewer but larger crystals grow after centrifugation of the protein sample. Crystals in (*b*) have a deeper orange colour than those in (*a*) owing to their size and thickness. (*c*) demonstrates the colour change from deep orange to pale yellow as a result of ageing crystals for more than four weeks. Both crystal size and age proved critical for obtaining well diffracting crystals. (*d*) shows a crystal with approximate dimensions of 0.1 × 0.1 × 0.05 mm mounted in an X-ray diffraction loop.

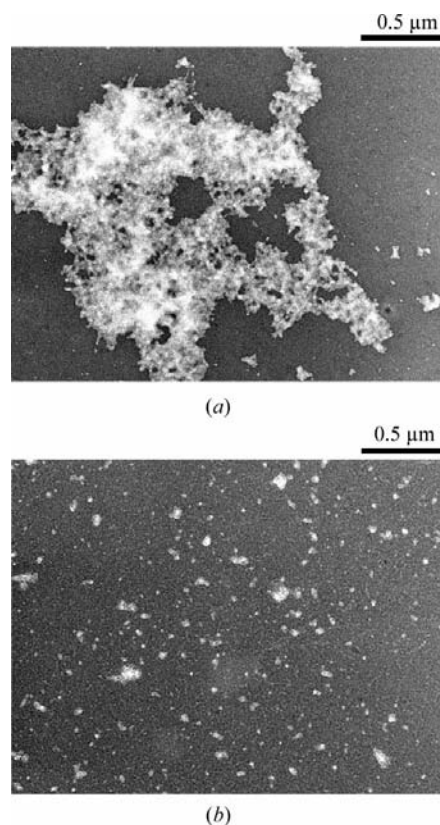


Figure 2
Sample-quality comparison by negative-stain electron microscopy of uncentrifuged (*a*) and centrifuged (*b*) protein sample. Large protein aggregates were removed by centrifugation of the protein sample and the sample became more homogeneous.

30 min), which resulted in removal of protein aggregates prior to crystallization trials.

2.5. Optimization of crystallization conditions

Crystals from the initial condition were small and diffracted very poorly. Screening for an alternative buffer type, pH and PEG concentration improved the size and diffraction quality of the crystals. Additive Screen 1 from Hampton Research was used for further optimization; 1 μ l of each additive was mixed with 9 μ l of reservoir solution and used to prepare drops as described above. The final optimized crystallization condition after iterative optimization cycles was 0.1 M Tris-HCl pH 8.2, 0.2 M CaCl₂, 29% PEG 400, 0.01 M BaCl₂, 3% ethylene glycol.

2.6. X-ray data collection

Crystals were frozen for X-ray data collection within 72 h of crystallization trial set-up. The crystals could be directly frozen from the drop since the condition contained sufficient cryoprotectants. Diffraction data

to 2.6 Å resolution were collected at beamline X06SA at the Swiss Light Source (SLS), Switzerland using a MAR 165 CCD detector. Data-collection statistics are summarized in Table 1. Image data were processed using the programs *DENZO* and *SCALEPACK* (Otwinowski & Minor, 1997). All data better than $-3.0\sigma(I)$ were used for scaling.

3. Results and discussion

An initial crystallization condition was identified using a commercially available screen. Initial crystals only diffracted to 5 Å. Both size and diffraction resolution of the crystals were then improved by optimization of the crystallization condition. Additive screening identified that barium chloride and ethylene glycol are very effective in improving the crystal quality. The ethylene glycol may confer an extra protective effect during the freezing process. Further optimization was achieved by controlling crystal nucleation. Following additive screening, each crystallization drop contained many small crystals, which only diffracted X-rays weakly (50 μ m along the longest length, 3.5–4 Å) (Fig. 1*a*). The large number of crystals in each drop rapidly depleted the protein concentration, limiting the final size of each crystal. To reduce the number of nucleations, the protein sample was centrifuged (175 000g for 30 min). The quality of the sample was checked by negative-stain electron microscopy before and after centrifugation; it was evident that this procedure removed protein aggregates (Fig. 2), making the protein sample more homogenous and limiting the number of nucleations. The crystals obtained from the centrifuged protein sample were larger (up to 150 μ m along the longest axis; Fig. 1*b*) and diffracted to a higher resolution. All further protein samples were subjected to centrifugation prior to crystallization trial set-up.

It proved critical to freeze the crystals within 72 h of crystallization set-up. Crystals that were frozen after this time limit showed no diffraction. This alteration in properties was apparent by the change in colour from deep orange to pale yellow that was observed in crystals more than four weeks old (Fig. 1*c*). The deep orange colour of the crystals is attributed to the presence of haem *b* within the protein. The loss or breakdown of haem, demonstrated by the change of colour in the crystals, could lead to structural instability and consequently loss of diffraction.

The new crystals of SQR belong to the trigonal space group R32, with unit-cell parameters $a = b = 138.7$, $c = 521.9$ Å. A native data set has been collected from one of the largest crystals (Fig. 1*d*). The majority of images clearly show diffraction to 2.6 Å. The data were processed and scaled to 2.6 Å resolution, as summarized in Table 1.

The optimization of the sample preparation and crystallization conditions for SQR from *E. coli*, which includes rational screening, electron microscopy and centrifugation, has resulted in crystals that yield data of sufficient resolution and quality to allow the structure of the protein to be solved. Structural determination by the multiwavelength anomalous dispersion (MAD) technique using the ten intrinsic Fe atoms per monomer is currently in progress. This structure will give further insights into the mechanism of this important respiratory complex.

This research was supported by the Biotechnology and Biological Sciences Research Council and Syngenta (RH/SI). It was also supported by the Department of Veterans' Affairs and National Institutes of Health grant GM61606 (VY/GC) and the Leverhulme Trust (ES/JB). We would like to thank Takashi Tomizaki and Clemens Schulze-Briese at SLS for technical assistance with data collection, and Tina Iverson and Mika Jormakka for comments.

References

- Baysal, B. E., Rubinstein, W. S. & Taschner, P. E. (2001). *J. Mol. Med.* **79**, 495–503.
- Cecchini, G., Schröder, I., Gunsalus, R. P. & Maklashina, E. (2002). *Biochim. Biophys. Acta*, **1553**, 140–157.
- Ishii, N., Fujii, M., Hartman, P. S., Tsuda, M., Yasuda, K., Senoo-Matsuda, N., Yanase, S., Ayusawa, D. & Suzuki, K. (1998). *Nature (London)*, **394**, 694–697.
- Iwata, S., Lee, J. W., Okada, K., Lee, J. K., Iwata, M., Rasmussen, B., Link, T. A., Ramaswamy, S. & Jap, B. K. (1998). *Science*, **281**, 64–71.
- Luna-Chavez, C., Iverson, T. M., Rees, D. C. & Cecchini, G. (2000). *Protein Expr. Purif.* **19**, 188–196.
- Maklashina, E., Berthold, D. A. & Cecchini, G. (1998). *J. Bacteriol.* **180**, 5989–5996.
- Matthews, B. W. (1968). *J. Mol. Biol.* **33**, 491–497.
- Ostermeier, C., Iwata, S., Ludwig, B. & Michel, H. (1995). *Nature Struct. Biol.* **2**, 842–846.
- Otwinowski, Z. & Minor, W. (1997). *Methods Enzymol.* **276**, 307–326.
- Spencer, M. E. & Guest, J. R. (1973). *J. Bacteriol.* **114**, 563–570.
- Törnroth, S., Yankovskaya, V., Cecchini, G. & Iwata, S. (2002). *Biochim. Biophys. Acta*, **1553**, 171–176.